CONCENTRATION LIMITS OF HYDROGEN–AIR–INHIBITOR DETONATIONS

S. M. Frolov and S. N. Medvedev

One-dimensional (1D) theory of detonability limits has been applied for mathematical modeling of chemical inhibiting of hydrogen–air detonations. The theory was shown to be capable of predicting the main specific features of the effect of chemical inhibitors on the concentration limits of hydrogen–air detonations in straight round tubes of different diameters at different initial pressures and temperatures. The detailed reaction mechanism of hydrogen oxidation has been used. Small additives of propene were shown to affect the chain-branching process by a fast reaction with active hydrogen atoms and reactions of propene regeneration leading to effective chain termination.

1 INTRODUCTION

Since the discovery of the detonation phenomenon, it is known that a steady self-sustained propagation of detonation waves in tubes is possible only within a certain range of explosive mixture composition, i. e., between fuel-lean and excessively fuel-rich one. Marginal values of fuel concentration were referred to as "concentration limits of detonability." It was found experimentally that the concentration limits are dependent of tube diameter, shape of tube cross section, initial pressure and temperature, as well as inert diluents and chemically active additives. Moreover, the limits are affected by introduction of mechanical obstructions (e. g., wall roughness, dispersed particles), additives exhibiting phase transition (e. g., water fog, film, or foam), by imposing electric fields, and even by elasticity of tube walls. Here, we restrict ourselves by considering the effect of chemical inhibitors on the concentration limits of hydrogen–air detonations.

Ideas on chemical inhibiting of hydrogen–air detonations were put forward long ago at testing piston engines operating on hydrogen [1]. As detonation suppression additives, methane, iodine, iodine hydrogen, organic iodeeds, as well as various metalorganic and nitrogen-organic compounds were considered. The effect of detonation suppression additives on the detonation properties of hydrogen–air mixtures were explained mostly by the low-temperature reactions of chain termination [2].

The search for effective detonation suppression additives has been revived recently in view of new developments in hydrogen technologies, in particular, fuel cells. Recent experimental studies [3–5] demonstrate that small additives of unsaturated hydrocarbons with π-bonds at the third carbon atoms (e. g., propene or iso-butylene) to hydrogen–air mixtures allow one to narrow considerably the concentration limits of detonation, to increase the predetonation run-up distance, and even to destroy the developed detonation wave. It has been concluded in these studies that inhibiting of hydrogen–air detonations with such additives is caused by termination of high-temperature chain-branching oxidation reactions.

Modern understanding of detonability limits is based on Zel'dovich article [6]. Zel'dovich was the first to consider momentum and energy losses intrinsic to confined reactive flows. In his 1D theory, concentration limits of detonability are attained because of competition between the rates of chemical energy release and losses. At the marginal fuel concentration, losses prevail and chemical energy release appears to be insufficient to support self-sustained propagation of a detonation wave. Contrary to the pre-Zel'dovich theories, where the concentration limits of detonability were explained by "available chemical time" to truncate chemical energy release in a detonation wave, in the Zel'dovich theory the "available chemical time" arises naturally.

In [6], Zel'dovich considered momentum and energy losses caused by skin friction at and heat transfer to the tube walls. The theory was later modified in [7–9] to incorporate realistic expressions for losses and cover the evolution of an explosive mixture from the initial state prior compression in a lead shock wave to the final state of stagnant and cooled combustion products.

In [9–12], the theory was extended qualitatively to tubes with rough walls. It was shown that mechanical obstructions can significantly widen detonability limits due to transition from the bulk ignition and reaction mechanism in the detonation wave to the mechanism of reflection-induced localized ignition with further turbulent flame propagation.

Quantitative applications of the theory to tubes with smooth walls were undertaken in [13, 14] and for tubes with rough walls in [15]. The generalized description of this and other available theories and their outcomes is provided elsewhere [16, 17].

The capabilities of the Zel'dovich theory of detonability limits have been comprehensively studied in [14] using the detailed kinetic mechanism of hydrogen oxidation and properly corrected values of heat transfer and skin friction coefficients at tube walls. The theory proved to provide satisfactory quantitative predictions for detonability limits depending on mixture composition, initial temperature and pressure, as well as the percentage of inert diluents in hydrogen–air mixture.

The objective of this work is to apply the model of [14] to the problem of chemical inhibiting of hydrogen–air detonations by small additives of effective gaseous detonation suppression agents.

2 STATEMENT OF THE PROBLEM

2.1 Phenomenology

Consider the propagation of a planar steady-state detonation wave in the straight round tube of diameter d uniformly filled with a premixed explosive gas. The simplifying assumptions adopted in the model are the same as in [14], namely:

(1) the flow behind the detonation wave is 1D;

(2) the structure of the detonation wave corresponds to the Zel'dovich – von Neumann – Döring (ZND) model;

(3) the reactive mixture obeys the ideal gas law;

(4) tube walls are isothermic;

(5) variation of flow parameters in the transversal direction is taken into account by skin friction and heat transfer coefficients at tube walls;

(6) skin friction and heat transfer coefficients are related trough Reynolds analogy;

(7) radiation effects are negligible; and

(8) the rate of chemical reaction is uniform in tube cross section.

Figure 1 shows the schematic of the flow in the frame of reference attached to the leading shock wave. The x-axis is directed downstream. The origin of coordinate ($x = 0$) is placed at the leading shock wave. According to the theory, the entire flow domain is divided into five zones: 1 to 5. From now on, all flow parameters in these zones will be denoted with indices 1 to 5. In the adopted frame of reference, the tube wall moves at detonation velocity D and possesses temperature T_1.

Zone 1 corresponds to the uniform initial mixture with density ρ_1, pressure p_1, temperature T_1, moving at the detonation velocity D.

Zone 2 is the reaction zone where the initial mixture first undergoes instantaneous adiabatic compression in the shock wave with the increase in density, pressure, and temperature from ρ_1, p_1, and T_1 to $\rho_2 = \rho_s$, $p_2 = p_s$, and $T_2 = T_s$ (index s denotes the parameters at the shock front) and decrease in flow velocity from D to u_s, while u_s is always less than the local sound velocity a_s: $u_s < a_s$. Thereafter, the mixture autoignites with a certain induction period and burns out gradually. As is known, heat deposition to the subsonic flow results in its acceleration: flow velocity increases up to $u_2 = u_{\mathrm{CJ}}$ (index CJ denotes parameters in the Chapman–Jouguet (CJ) plane). In the CJ plane, an important condition is met: gas velocity is equal to the local sound velocity: $u_{\mathrm{CJ}} = a_{\mathrm{CJ}}$. This

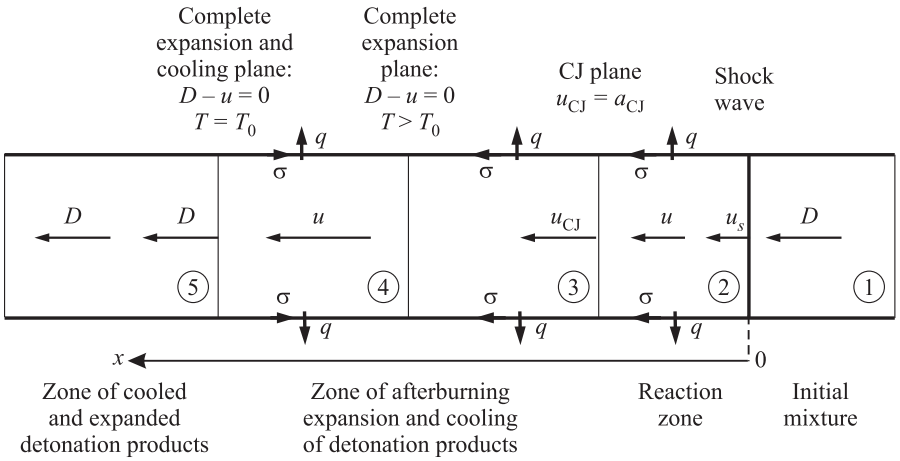

Figure 1 Structure of 1D steady-state detonation wave

condition ("CJ condition") determines the stability of the detonation wave since small perturbations originating downstream from the CJ plane do not penetrate into the reaction zone. The gas temperature in the reaction zone increases up to $T_2 = T_{CJ}$, whereas its density and pressure decrease to $\rho_2 = \rho_{CJ}$ and $p_2 = p_{CJ}$. Due to the fact that temperature T_2 is higher than wall temperature T_1, there is a heat flux q from the reaction zone to the tube wall, i. e., the flow in zone 2 is nonadiabatic. Moreover, since $u_2 < D$, the tube wall produces "external" work over the gas due to nonzero viscous friction σ directed downstream as shown in Fig. 1. Contrary to the chemical energy release, heat withdrawal from and "external" work over the gas result in the deceleration of the subsonic flow, i. e., impede the meeting of the CJ condition, and actually determine the existence of detonability limits. The factors impeding the meeting of the CJ condition in the reaction zone of a detonation wave are often referred to as "losses" in the literature. In the specific case under consideration, one deals with the momentum and heat losses. Note that due to the competing effects of different physical and chemical processes in the reaction zone, chemical transformation in the CJ plane is, in general, incomplete.

In zones 3 and 4, the mixture not reacted in zone 2 burns out and the detonation products expand and cool down. In zone 3, the supersonic flow accelerates from $u_3 = u_{CJ}$ to $u_3 = D$ under the action of "external" work of the tube wall and heat removal to the tube wall, i. e., the flow completely expands from the elevated density $\rho_3 = \rho_{CJ}$ to the initial density $\rho_3 = \rho_1$. Of course, mixture afterburning in zone 3 somehow resists to the acceleration of the supersonic flow. Since the gas temperature at the end of zone 3 still differs from the wall tem-

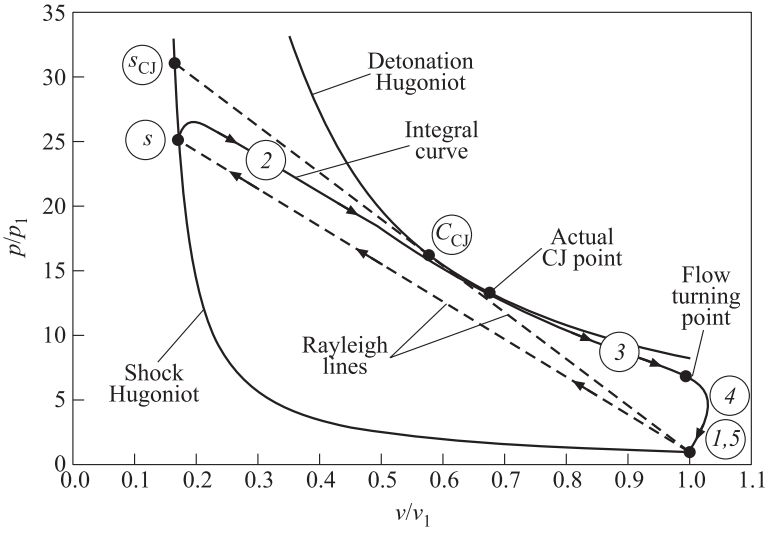

Figure 2 Variation of mixture state in the detonation wave at the pressure – specific volume plane

perature ($T_3 > T_1$), the cooling of the detonation products continues. In zone 4, the supersonic flow first continues accelerating up to the velocity $u_4 > D$ due to the dominant effect of cooling but then decelerates to velocity $u_4 = D$ due to the dominant effect of viscous friction at the tube wall. The stress vector of viscous friction changes its direction to the opposite in zone 4 due to the condition $u_4 > D$ (see Fig. 1).

In zone 5, the detonation products attain the density and temperature of the initial mixture and move at velocity D. Pressure in zone 5 can be somewhat different from p_1, if the number of moles in the course of chemical reactions has been changed.

In Fig. 2, the arrows schematically show the variation of mixture state in the detonation wave at the "pressure – specific volume" plane. As a result of losses, the state of the gas varies along curve *1–s–2–3–4–5*, with the stepwise transition from state *1* to state *s*. Remind that in the theory of ideal ZND detonation, the state of the gas varies along the straight Rayleygh line *1*–s_{CJ}–C_{CJ}, where C_{CJ} is the classical CJ point (state) which is the tangent point of the detonation Hugoniot and the Raylegh line. At the existence of momentum and heat losses, the actual CJ point lies below and to the right from the classical CJ point, and, in general, it does not lie at the detonation Hugoniot for the thermodynamically equilibrium detonation products at specified initial conditions.

Thus, the flow region occupied by the detonation wave is represented by zones 2, 3, and 4. For solving the problem of chemical inhibiting of hydrogen–air

detonations by small additives of effective detonation suppression agents, one generally has to consider the flow in all these zones.

2.2 Mathematical Statement

Presented below are the governing equations of model [14]:

– continuity equation for the mixture:

$$\frac{d\rho u}{dx} = 0\,; \tag{1}$$

– continuity equations for individual chemical species:

$$\frac{d\rho_i u}{dx} = w_i \mu_i\,; \quad \rho_i = c_i \mu_i \tag{2}$$

where

$$w_i = \sum_{j=1}^{L} \beta_{ij} r_j\,; \quad r_j = k_f \prod_{l=1}^{n} c_l - k_r \prod_{l=1}^{m} c_l\,;$$

– momentum conservation equation for the mixture:

$$\frac{d}{dx}\left(p + \rho u^2\right) = \frac{\Pi}{\Phi}\,\sigma\,; \tag{3}$$

– energy conservation equation for the mixture:

$$\rho u \frac{d}{dx}\left(\frac{u^2}{2} + \frac{\sum\limits_{i=1}^{N} H_i c_i}{\rho}\right) = \frac{\Pi}{\Phi}\,(\sigma D - q)\ . \tag{4}$$

In Eqs. (1)–(4), c_i, μ_i, and H_i are the molar concentration, molecular mass, and enthalpy (including a chemical part) of the ith chemical species in the mixture; L is the total number of chemical reactions in the mixture; β_{ij} is the stoichiometric coefficient for the ith species in the jth reaction; N is the total number of chemical species in the mixture; k_f and k_r are the rate constants of the forward and reverse reactions; and Π and Φ are the perimeter and cross section of the tube, respectively.

The rate constants k_f and k_r are determined from the relationship:

$$k = AT^n \exp\left(-\frac{E}{RT}\right) \tag{5}$$

where E is the activation energy; A is the preexponential factor; and n is the power exponent.

The set of Eqs. (1)–(4) is supplemented by the ideal gas equation of state:

$$p = \sum_{i=1}^{N} \rho_i RT \tag{6}$$

where R is the gas constant. In addition, the following relationships for the skin friction σ and heat flux q are used:

$$\sigma = \frac{1}{2} C_f \rho (D-u) |D-u| , \quad C_f = \frac{0.3164}{\mathrm{Re}^{0.25}} ; \tag{7}$$

$$q = C_h \rho (D-u) \left[C_p (T - T_1) + \frac{1}{2} (D-u)^2 \right] , \quad C_h = \frac{1}{2} C_f . \tag{8}$$

In Eqs. (7) and (8), C_f is the skin friction coefficient determined by Blasius formula; C_h is the dimensionless heat transfer coefficient determined based on the Reynolds analogy; C_p is the specific heat at constant pressure; and Re is the Reynolds number determined as

$$\mathrm{Re} = \frac{\rho_1 |D-u| d}{\eta_1} \tag{9}$$

where η_1 is the mixture dynamic viscosity [18]:

$$\eta_1 = \frac{26.7 \cdot 10^{-7} (\mu_1 T_1)^{0.5}}{\sigma_m^2} \tag{10}$$

with σ_m denoting molecule "radius" in the mixture within the model of rigid spheres and μ_1 denoting the molecular mass of the mixture.

For solving differential Eqs. (1)–(4), one has to specify boundary conditions at the shock front ($x = 0$) and at a large distance from the shock front ($x \to \infty$). The boundary conditions at the shock front correspond to the Rankine–Hugoniot conditions:

$$\left.\begin{gathered} \rho_s u_s = \rho_1 D ; \\ p_s + \rho_s u_s^2 = p_1 + \rho_1 D^2 ; \\ \frac{1}{\rho_s} \left(\sum_{i=1}^{N} H_i c_i \right)_s + \frac{u_s^2}{2} = \frac{1}{\rho_1} \left(\sum_{i=1}^{N} H_i c_i \right)_1 + \frac{D^2}{2} ; \\ (c_i)_s = (c_i)_1 . \end{gathered}\right\} \tag{11}$$

At a large distance from the shock front, the following conditions should be met:

$$x \to \infty : \quad \rho \to \rho_1 ; \; T \to T_1 . \tag{12}$$

In this mathematical statement, the detonation velocity D is the problem eigenvalue which should be found by the shooting technique [9].

2.3 Reaction Mechanism

For describing the effect of chemical inhibitor on hydrogen–air detonations, one has to apply the reaction mechanisms taking into account the main stages of chain-branching process of hydrogen oxidation with known reaction rate constants and thermochemical data.

Table 1 shows the reaction mechanism of hydrogen oxidation used in this work. The mechanism contains 21 reactions (I to XXI) with 8 species (H_2, O_2, OH, H_2O, H, O, HO_2, and H_2O_2). Third body partner M in the table denotes any third species in the mixture. All required thermochemical data were taken from [19]. Propene (C_3H_6) has been chosen as the detonation inhibitor. The effect of propene is modeled by two reactions supplementing the mechanism of Table 1:

$$C_3H_6 + H\ (+M) \rightarrow C_3H_7\ (+M) \qquad \text{XXII}$$

and

$$C_3H_7 + O_2 \rightarrow C_3H_6 + H_2O\,. \qquad \text{XXIII}$$

Reaction XXII is the reaction of chain termination due to attraction of active hydrogen atom with the formation of considerably less active propyl radical C_3H_7. Due to high frequency of triple collisions at atmospheric and elevated pressures, reaction XXII proceeds with the second kinetic order. The rate constant of reaction XXII is [20]:

$$k = 1.3 \cdot 10^{10} \exp\left(-\frac{787.87}{T}\right)\ (\mathrm{l, mole, s}) \qquad (13)$$

Comparison of reaction rate constants for reactions XXII and III shows that addition of propene to hydrogen–air mixture in the amount on the order of tenth fraction of percent leads to effective competition between the chain termination reaction XXII and chain-branching reaction III. Note that propene reacts not only with atomic hydrogen (reaction XXII) but also with other active chain carriers — atomic oxygen O and OH radical. Therefore, the account of only one reaction XXII actually underestimates the rate of chain termination as the reactions between C_3H_6, O, and OH result in the replacement of active chain carriers by less active radicals not capable to continue reaction chains.

Reaction XXIII is the reaction of propene regeneration due to interaction between propyl radical with molecular oxygen. The rate constant of reaction XXIII is [21]:

$$k = 1.26 \cdot 10^{8}\ (\mathrm{l, mol, s})\,. \qquad (14)$$

Table 1 Reaction mechanism of hydrogen oxidation [14]

No.	Reaction	Forward reaction			Reverse reaction		
		$\lg A$, cm, mole, s	n	E, kcal/mole	$\lg A$, cm, mole, s	n	E, kcal/mole
I	$H_2 + O_2 = OH + OH$	13.24	0	48.1	10.82	0.3	29.2
II	$OH + H_2 = H_2O + H$	8.00	1.6	3.30	8.66	1.6	18.57
III	$H + O_2 = OH + O$	17.08	−0.9	16.52	13.25	0	0
IV	$O + H_2 = OH + H$	7.18	2.0	7.55	3.69	2.8	3.88
V	$O + H_2O = OH + OH$	10.18	1.1	17.26	9.18	1.1	0
VI	$H + H + M = H_2 + M$	17.81	−1.0	0	18.77	−1.1	104.4
VII	$H + O_2 + M = HO_2 + M$	17.85	−0.8	0	19.06	−1.2	48.41
VIII	$OH + H + M = H_2O + M$	21.92	−2.0	0	15.11	0	105.1
IX	$HO_2 + H_2 = H_2O_2 + H$	13.48	0	26.03	13.68	0	7.95
X	$HO_2 + HO_2 = H_2O_2 + O_2$	12.26	0	0	13.73	0	39.74
XI	$H + HO_2 = OH + OH$	14.40	0	1.9	13.08	0	40.1
XII	$H + HO_2 = H_2O + O$	13.15	0	2.08	12.74	0	57.53
XIII	$H + HO_2 = H_2 + O_2$	13.82	0	2.13	14.16	0	56.64
XIV	$O + HO_2 = OH + O_2$	13.24	0	−0.4	13.35	0	52.66
XV	$OH + HO_2 = H_2O + O_2$	13.48	0	0	14.60	0	73.0
XVI	$OH + OH + M = H_2O_2 + M$	24.76	−3.0	0	33.11	−4.9	53.25
XVII	$HO_2 + H_2 = H_2O + OH$	11.78	0	18.68	11.44	0	73.74
XVIII	$HO_2 + H_2O = H_2O_2 + OH$	13.40	0	32.29	13.06	0	1.76
XIX	$H + H_2O = H_2O + OH$	13.38	0	3.97	14.06	0	79.19
XX	$OH + M = O + H + M$	15.38	0	99.36	18.67	−1.0	0
XXI	$O + O + M = O_2 + M$	13.28	0	−1.79	18.26	−1.0	118.1

2.4 Numerical Approach

Nonlinear differential Eqs. (1)–(4) and additional relationships (5)–(14) were transformed to the dimensionless form using the following notations:

$$S = \frac{dv_1}{a_1^2}\frac{\Pi}{\Phi}\sigma\,; \quad W = \frac{dv_1}{a_1^2 D}\frac{\Pi}{\Phi}q\,; \quad \mathrm{M} = \frac{D}{a_1}\,;$$
$$P = \frac{p}{p_1}\,; \quad V = \frac{v}{v_1}\,; \quad \tau = \frac{a_1}{d}\,t\,; \quad \xi = \frac{X}{d}$$

where v_1 and a_1 are the specific volume and sound velocity of the mixture in zone 1 (see Fig. 1).

In the dimensionless form, the set of governing equations can be rewritten as

$$\frac{dV}{d\xi} = \frac{1}{\mathrm{M}^2}\frac{f' - f''}{\psi}\,; \quad \frac{dP}{d\xi} = \gamma_1\frac{f' - f''(1-\psi)}{\psi} \tag{15}$$

where

$$\psi = 1 - \frac{P\sum\left((H_i/(RT))c_i v\right)}{\gamma_1 \mathrm{M}^2 V}\,; \quad f' = S\,;$$

$$f'' = (\gamma - 1)\left(S\frac{1-V}{V} - \frac{W}{V}\right) - \\ - (\gamma - 1)\frac{PV}{C_1 \mathrm{M} V^2}\sum w_i v\left(\frac{H_i}{RT} - \frac{v\sum c_i(C_{P_i}/R)}{v\sum c_i}\right).$$

Here, parameters S and W correspond to the power of momentum and heat losses, respectively.

Variable $\varphi = f' - f''$ is proportional to the difference between the power of chemical energy release and power of losses, whereas variable ψ is proportional to the difference between the local values of flow velocity and sound velocity. The conditions when variables φ and ψ become simultaneously equal to zero, i. e.,

$$\frac{dV}{d\xi} = \frac{0}{0}\,; \quad \frac{dP}{d\xi} = \frac{0}{0}\,, \tag{16}$$

correspond to the generalized CJ condition first suggested by Zel'dovich [6, 7]. The singularity point 0/0 in Eqs. (16) is of the saddle type. For solving the problem with boundary conditions (12), one has to ensure continuous transition through the singularity point to the supersonic flow zone 3 (see Fig. 1). Such a transition is possible only at a certain value of detonation velocity D. Therefore, instead of boundary conditions (12), the condition of continuous transition through the singularity point was used.

Similar to [14], the value of detonation velocity D was determined by the shooting technique, i. e., by integrating the set of Eqs. (15) jointly with the kinetic equations and additional relationships at different D until both conditions of Eq. (16) are met simultaneously. The problem was solved by the fourth order Runge–Kutta method. The set of kinetic equations was solved by the implicit method [22] with internal time stepping. The relative error of determining the detonation velocity did not exceed 0.05%.

3 RESULTS

3.1 Detonability Limits

Effect of inhibitor on the structure and concentration limits of hydrogen–air detonations was considered on the example of small (1 %(vol.) and 2 %(vol.)) propene (C_3H_6) additives. The concentrations of propene considered are lower than the low flammability limit in the mixtures under study in the absence of hydrogen (at initial temperature 293 K). However, at conditions of hydrogen combustion, the hydrocarbon is getting involved into reactions with atoms and radicals formed in the hydrogen flame. As a result, oxygen is partly consumed in the reactions with radicals formed from C_3H_6 molecules.

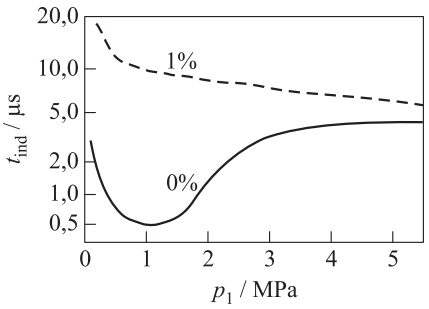

Figure 3 Predicted ignition delay time as a function of initial pressure for the stoichiometric H_2 + air mixture with 1 %(vol.) (curve 1%) and without (curve 0%) propene additive at initial temperature $T_1 = 1200$ K

The effect of detonation inhibitor is manifested by the elongation of ignition induction period t_{ind}. In the calculations, the induction period was defined as the time taken for the temperature growth rate to attain the value of 10^7 K/s.

Figure 3 shows the predicted dependencies of t_{ind} on the initial pressure for the stoichiometric hydrogen–air mixture with (curve 1%) and without (curve 0%) propene additive at $T_1 = 1200$ K. Curve "1%" is seen to qualitatively differ from curve "0%." For the mixture with inhibitor, the ignition delay time decreases monotonically with pressure at least within a pressure range $p_1 = 0.1$–5.0 MPa. At pressure exceeding 5.0 MPa, the curves are getting closer, i.e., the efficiency of the inhibitor decreases.

Figures 4*a* and 4*b* show the predicted time histories of temperature and atomic hydrogen concentration for the conditions of Fig. 3 at initial pressure

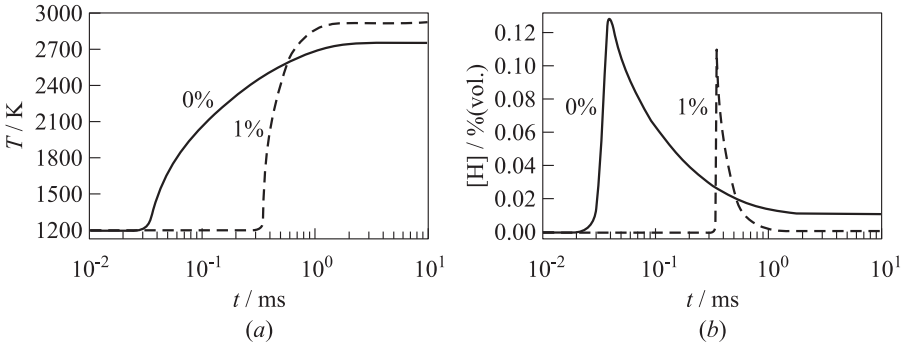

Figure 4 Predicted time histories of temperature (a) and atomic hydrogen concentration (b) for autoignition of 29.6% H_2 + 70.4% air (curve "0%") and 29.6% H_2 + 1.0% C_3H_6 + 69.4% air (curve "1%") at $p_1 = 0.1$ MPa and $T_1 = 1200$ K

0.1 MPa. The ignition induction times are seen to differ by the order of magnitude. The final temperature of the combustion products of the mixture with inhibitor is about 200 K higher than that of the pure hydrogen–air mixture, which is caused by exothermic reactions XXII and XXIII. Curve "1%" in Fig. 4b indicates that the maximum concentration of atomic hydrogen is about 20% lower than in the mixture without inhibitor. Moreover, in the mixture with inhibitor, atomic hydrogen exists in appreciable amounts for considerably shorter time than in the mixture without inhibitor.

Figure 5 shows the predicted time histories of $[C_3H_6]$ concentrations at autoignition of the stoichiometric hydrogen–air mixture with and without inhibitor. The behavior of the "$[C_3H_6]$" curve during the induction period looks like no reactions with $[C_3H_6]$ virtually occur. However, Fig. 5 shows that in the mixture with inhibitor, formation and accumulation of propyl radical $[C_3H_7]$ occurs from the very beginning, which is the indication of reaction between $[C_3H_6]$ and atomic hydrogen — one of the main carriers of chain-branching process. Inhibitor is regenerated producing $[HO_2]$ radical. For the sake of comparison, Fig. 5 displays the kinetic curve for $[HO_2]$ radical in the mixtures with and without inhibitor.

Addition of inhibitor to hydrogen–air mixture results in narrowing of concentration limits and increasing the limiting tube diameter for the detonation.

Figure 6 shows the predicted dependencies of the limiting tube diameter on hydrogen concentration in the mixture with 0%, 1%, and 2% propene additives. The predicted limiting tube diameter for pure hydrogen–air mixtures (curve "0%") is compared with direct measurements (diamonds [23]). A satisfactory quantitative agreement between predictions and measurements is worth mentioning. As is seen from Fig. 6, addition of 1% propene to the hydrogen–air

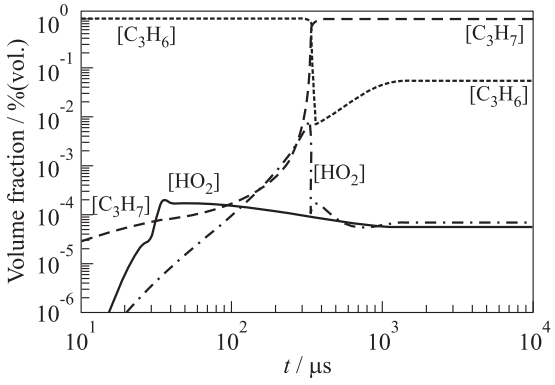

Figure 5 Predicted time histories of C_3H_6, C_3H_7, and HO_2 concentrations at autoignition of 29.6% H_2 + 70.4% air (broken curves) and 29.6% H_2 + 1.0% C_3H_6 + 69.4% air (solid curve) mixtures at $p_1 = 0.1$ MPa and $T_1 = 1200$ K

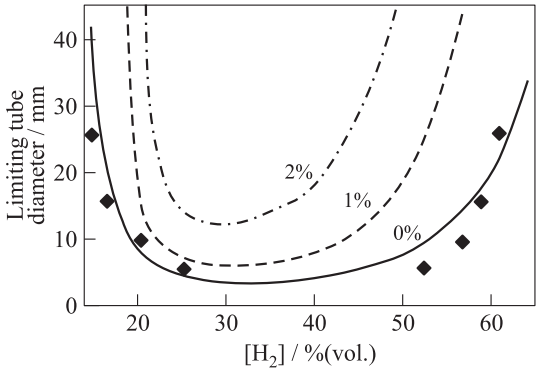

Figure 6 Limiting tube diameter as a function of hydrogen concentration in hydrogen–air mixture. Curves "0%," "1%," and "2%" correspond to different percentage (vol.) of propene in the mixture. Initial parameters: $p_1 = 0.1$ MPa and $T_1 = 298$ K. Diamonds show the results of direct experiments [23] for pure hydrogen–air mixtures

mixture results in shifting the fuel-lean detonability limit in the tube 20 mm in diameter from 16.9 to 19.76 %(vol.) and the fuel-rich detonability limit from 60.05 to 50.63 %(vol.). Addition of 1 %(vol.) propene to the mixture results in increasing the minimal limiting tube diameter from 3.7 mm (without inhibitor) to 6.3 mm, whereas addition of 2 %(vol.) propene increases the minimal limiting tube diameter to 12.5 mm. Also, addition of inhibitor shifts the minimum of the

U-shaped curves in Fig. 6 towards mixture compositions with lower hydrogen content.

One more important observation comes from Fig. 6. Even in tubes of very large diameter where the effect of momentum and heat losses on detonation parameters can be neglected, propene additives affect the concentration detonability limits. As a matter of fact, addition of 1 %(vol.) inhibitor results in shifting the fuel-lean and fuel-rich concentration limits by approximately 3 and 8 %(vol.), respectively, in terms of H_2 concentration. Addition of 2 %(vol.) inhibitor results in shifting these detonability limits by 6 and 16 %(vol.), respectively.

The computational results with the nonzero concentration of inhibitor agree qualitatively with recent experimental findings [5]. For quantitative comparison of calculations with experiments, a more detailed treatment of inhibitor reaction kinetics is required.

3.2 Detonation Structure

Consider now the effect of chemical inhibitor on the 1D structure of hydrogen–air detonations.

Figure 7 shows the predicted time histories of temperature, specific volume, and concentrations of [H], [HO_2], and [H_2O_2] for the near-limiting detonation regimes in mixtures without inhibitor (curves "0%") and with "1%" inhibitor additive (curves "1%"). The diameters of the tubes used in the calculations are $d = 6$ and 9 mm, respectively. The results of calculations presented in Fig. 7 correspond to hydrogen–air mixture with 22 %(vol.) H_2 at $T_1 = 298$ K and $p_1 = 0.1$ MPa. The difference in the temperature at the leading shock front at curves "0%" and "1%" is caused by the difference in the steady-state detonation velocities equal to $D = 1681.5$ m/s for curves "0%" and $D = 1748.4$ m/s for curves "1%." The temperature in the CJ point for curves "1%" in Fig. 7 is higher than for curves "0%" due to the high formation enthalpy of inhibitor. In general, in both cases, the temperature histories are qualitatively similar. As for the behavior of intermediate reaction products (H, HO_2, and H_2O_2), Fig. 7 demonstrates that in the mixture with inhibitor, the concentration of atomic hydrogen is lower, whereas the concentrations of less active species HO_2 and H_2O_2 are considerably higher than in the mixture without inhibitor.

Figure 8 shows the predicted dependencies of the detonation velocity deficit on hydrogen concentration in the mixture without and with 1% propene additive. As is seen, for the pure hydrogen–air mixture, the detonation velocity in the vicinity to detonability limits differs from the ideal CJ value only slightly, i. e., $\Delta D/D_{\mathrm{CJ}} = 4\%$–$5\%$ at the fuel-lean limit and $\Delta D/D_{\mathrm{CJ}} = 8\%$–$10\%$ at the fuel-rich limit. The maximum allowable detonation velocity deficit ($\sim 15\%$) in this case is attained at 35–45 %(vol.) H_2. In the mixture with 1 %(vol.) inhibitor,

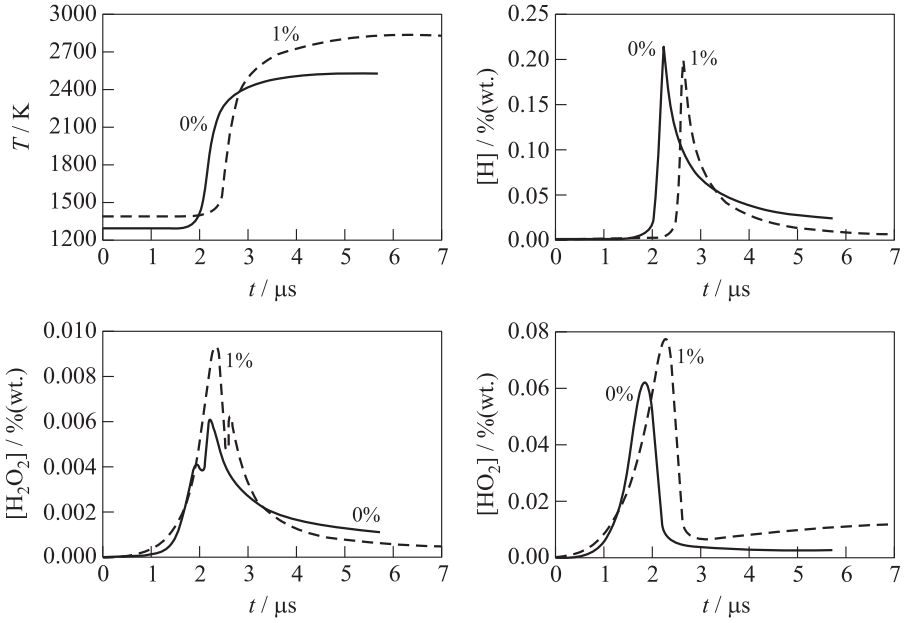

Figure 7 Predicted time histories of temperature and mass fractions of H, HO_2, and H_2O_2 in hydrogen–air–inhibitor detonations. Curves "0%" correspond to 22 %(vol.) H_2 + 78 %(vol.) air mixture. Curves "1%" correspond to 22 %(vol.) H_2 + 1 %(vol.) C_3H_6 + 77 %(vol.) air mixture. Initial parameters: $p_1 = 0.1$ MPa and $T_1 = 298$ K

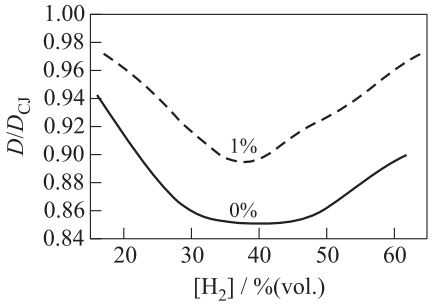

Figure 8 Predicted dependence of detonation velocity deficit on hydrogen concentration in H_2–air mixture. Curve "0%" corresponds to the mixture without inhibitor, curve "1%" corresponds to the mixture with 1% propene. Initial parameters: $p_1 = 0.1$ MPa and $T_1 = 298$ K

both concentration limits as well as the maximum allowable detonation velocity deficit decrease (curve "1%" in Fig. 8).

Thus, addition of 1 %(vol.) C_3H_6 decreases the maximum detonation velocity deficit at the fuel-lean limit to $\Delta D/D_{CJ} = 2\%$–3% and at the fuel-rich limit to 3%–4%, whereas the maximum allowable detonation velocity deficit becomes less than 11% and attained at 35–40 %(vol.) H_2 in the mixture.

4 CONCLUDING REMARKS

The applicability of 1D theory to detonation phenomena is often called in question. The reason is that the 1D structure of detonation is known to be inherently unstable. A realistic detonation wave exhibits a complex three-dimensional structure with transverse waves, shear layers, distributed induction and reaction zones and a 1D theory fails to resolve these particular details. Nevertheless, it is based on reasonable assumptions regarding averaging of flow parameters over a tube cross section and applies fundamental conservation laws.

The theory correctly reflects the comparative contribution of average hydrodynamic and thermochemical effects. There exists an impressive quantitative agreement of its predictions with experimental measurements of average detonation velocity and pressure. Moreover, detailed calculations for hydrogen–air mixtures (see [14] and Fig. 6 above) show that the 1D theory can provide correct quantitative predictions of detonability limits under a wide range of initial conditions, fuel concentration, and inert diluent.

In this paper, mathematical modeling of chemical inhibiting of hydrogen–air detonations has been performed using the 1D detonation model with due regard for detailed chain-branching reaction mechanism of hydrogen oxidation. The model was shown to describe satisfactorily all main effects of chemical inhibitors on the detonation.

The results of calculations indicate that chemical inhibitors narrow the concentration limits of detonations and increase the limiting tube diameter, in which the steady-state detonation propagation is still possible. Despite the inhibitors introduce additional exothermic reactions and additional hydrogen oxidation reactions, their presence results in detonation suppression.

Inhibitors lead to the deceleration of the overall reaction process which manifests itself by increased ignition delay time and decreased concentrations of atomic hydrogen — main carrier of chain-branching reaction. The effect of inhibitors is mainly determined by the specific dependence of the rate of chain-branching reaction on temperature which differs from the regular Arrhenius dependence.

ACKNOWLEDGMENTS

The authors thank Prof. V. V. Azatyan for fruitful discussions. This work was partly performed under RFBR grant 08-08-00068 and State contracts of Russian Federation Nos. П502 and 02.516.12.6026.

REFERENCES

1. Sokolik, A. S. 1960. *Selfignition, flame, and detonation in gases*. Moscow: USSR Academy of Sci. Publ.
2. Lewis, B., and G. Elbe. 1961. *Combustion, flames and explosions of gases*. N.Y.: Academic Press.
3. Azatyan, V. V., I. M. Naboko, V. A. Petukhov, *et al.* 2004. Chemical suppression of hydrogen–air explosion under conditions of cumulation at strong initiation of combustion. *Dokl. Phys. Chem.* 394(1):61–64.
4. Azatyan, V. V., V. A. Pavlov, and O. P. Shatalov. 2005. Inhibition of the combustion and detonation of hydrogen–air mixture behind the shock front. *Kinet. Catal.* 46(6):789–99.
5. Azatyan, V. V., D. I. Baklanov, I. S. Gordopolova, S. K. Abramov, and A. A. Piloyan. 2007. Inhibiting of stationary detonation waves in hydrogen–air mixtures. *Dokl. Phys. Chem.* 415(2):1–4.
6. Zel'dovich, Ya. B. 1940. To the theory of detonation propagation in gaseous systems. *JETP* 10(5):542.
7. Zel'dovich, Ya. B., and A. S. Kompaneets. 1955. *The theory of detonation*. Moscow: Gostekhteorizdat.
8. Zel'dovich, Ya. B., B. E. Gel'fand, Ya. M. Kazhdan, and S. M. Frolov. 1987. Detonation propagation in a rough tube taking account of deceleration and heat transfer. *Combust. Explosion Shock Waves* 23(3):342–49.
9. Zel'dovich, Ya. B., A. A. Borisov, B. E. Gelfand, S. M. Frolov, and A. E. Mailkov. 1988. Nonideal detonation waves in rough tubes. In: *Dynamics of explosions*. Eds. A. L. Kuhl, J. R. Bowen, J.-C. Leyer, and A. A. Borisov. Progress in astronautics and aeronautics ser. Washington, DC: AIAA Inc. 114:211–31.
10. Rybanin, S. S. 1969. Theory of detonation in rough tubes. *Combust. Explosion Shock Waves* 5(3):274–78.
11. Zel'dovich, Ya. B., B. E. Gelfand, A. A. Borisov, S. M. Frolov, and A. N. Polenov. 1985. Reaction zone in low-speed detonation in rough tubes. *Chem. Phys. Rep.* 4(2):279–88.
12. Frolov, S. M., B. E. Gelfand, and S. P. Medvedev. 1990. Calculation of the velocity of gaseous detonation in a rough tube based on measurements of shock wave attenuation. In: *Dynamics of detonations and explosions*. Eds. A. L. Kuhl, J.-C. Leyer, A. A. Borisov, and W. A. Sirignano. Progress in astronautics and aeronautics ser. Washington, DC: AIAA Inc. 133:241–55.

13. Frolov, S. M., and B. E. Gelfand. 1993. Limiting tube diameter of gaseous detonation. In: *Dynamic aspects of detonations*. Eds. A. L. Kuhl, J.-C. Leyer, A. A. Borisov, and W. A. Sirignano. Progress in astronautics and aeronautics ser. Washington, DC: AIAA Inc. 153:298–311.
14. Agafonov, G. L., and S. M. Frolov. 1994. Calculation of detonability limits for hydrogen-containing mixtures. *Combust. Explosion Shock Waves* 30(1):92–100.
15. Gelfand, B. E., S. M. Frolov, and M. A. Nettleton. 1991. Gaseous detonations — a selective review. *Progr. Energy Combust. Sci.* 17(4):327–71.
16. Frolov, S. M. 1995. On the Zel'dovich theory of detonability limits. In: *Combustion, Detonation, Shock Waves*. Proc. Zel'dovich Memorial. Eds. A. G. Merzhanov and S. M. Frolov. Moscow: ENAS Publ. 1:266–72.
17. Frolov, S. M. 1997. Zel'dovich theory of detonability limits. In: *Advances in combustion science: In honor of Ya. B. Zel'dovich*. Eds. W. A. Sirignano, A. G. Merzhanov, and L. De Luca. Progress in astronautics and aeronautics ser. Reston, VA: AIAA Inc. 173:341–47.
18. Reid, R., J. M. Prausnitz, and T. K. Sherwood. 1997. *The properties of gases and liquids*. N.Y.: McGrow Hill.
19. McBride, B. J., M. J. Zehe, and G. Sanford. 2002. *NASA Glenn coefficients for calculating thermodynamic properties of individual species*. Cleveland, Ohio: Glenn Research Center. 273 p.
20. Tsang, W. 1991. Chemical kinetic data base for combustion chemistry. Part V. Propen. *J. Phys. Chem. Ref. Data*. 221 p.
21. Warnatz, J. 1984. Rate coefficients in the C/H/O system. In: *Combustion chemistry*. Ed. W. C. Gardiner. N.Y.: Springer-Verlag. 197–361.
22. Polak, L. S., L. S. Goldenberg, M. Ya. Goldenberg, and A. A. Levitskii. 1984. *Computational methods in chemical kinetics*. Moscow: Nauka.
23. Pawel, D., H. Vasatko, and H. Gg. Wagner. 1967. The influence of temperature on the limits of detonability. Report AF EOAR 67-49. Gottingen: Inst. für Physikalishe Chemie.